



## OPEN ACCESS

## EDITED BY

Muwen Lu,  
South China Agricultural University,  
China

## REVIEWED BY

Junqing Huang,  
Jinan University, China  
Bowen Chang,  
The First Affiliated Hospital  
of University of Science  
and Technology of China Anhui  
Provincial Hospital, China

## \*CORRESPONDENCE

Guowei Le  
lgw@jiangnan.edu.cn

†These authors have contributed  
equally to this work and share first  
authorship

## SPECIALTY SECTION

This article was submitted to  
Nutrition and Food Science  
Technology,  
a section of the journal  
Frontiers in Nutrition

RECEIVED 08 September 2022

ACCEPTED 03 October 2022

PUBLISHED 08 November 2022

## CITATION

Jiang Y, Feng C, Shi Y, Kou X and Le G  
(2022) Eugenol improves high-fat  
diet/streptomycin-induced type 2  
diabetes mellitus (T2DM) mice muscle  
dysfunction by alleviating  
inflammation and increasing muscle  
glucose uptake.  
*Front. Nutr.* 9:1039753.  
doi: 10.3389/fnut.2022.1039753

## COPYRIGHT

© 2022 Jiang, Feng, Shi, Kou and Le.  
This is an open-access article  
distributed under the terms of the  
[Creative Commons Attribution License  
\(CC BY\)](https://creativecommons.org/licenses/by/4.0/). The use, distribution or  
reproduction in other forums is  
permitted, provided the original  
author(s) and the copyright owner(s)  
are credited and that the original  
publication in this journal is cited, in  
accordance with accepted academic  
practice. No use, distribution or  
reproduction is permitted which does  
not comply with these terms.

# Eugenol improves high-fat diet/streptomycin-induced type 2 diabetes mellitus (T2DM) mice muscle dysfunction by alleviating inflammation and increasing muscle glucose uptake

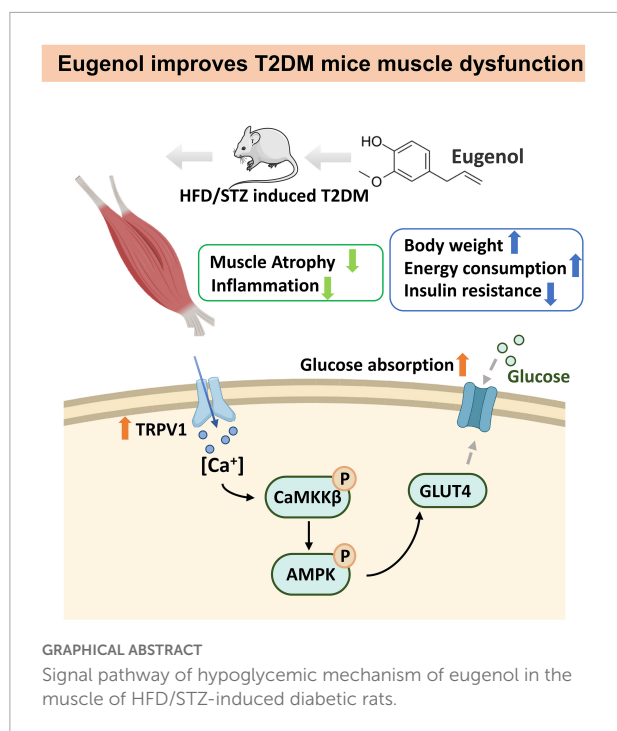
Yuge Jiang<sup>1,2†</sup>, Chuanxing Feng<sup>1,2†</sup>, Yonghui Shi<sup>1,2</sup>,  
Xingran Kou<sup>3</sup> and Guowei Le<sup>1,2\*</sup>

<sup>1</sup>Center for Food Nutrition and Functional Food Engineering, School of Food Science and Technology, Jiangnan University, Wuxi, China, <sup>2</sup>The State Key Laboratory of Food Science and Technology, Jiangnan University, Wuxi, China, <sup>3</sup>School of Perfume and Aroma Technology, Shanghai Institute of Technology, Shanghai, China

Eugenol has been used in dietary interventions for metabolic diseases such as diabetes and obesity. However, the protective effect of eugenol on muscle function in diabetes is unclear. In this study, a high-fat diet (HFD) with a streptozocin (STZ) injection induced type II diabetes mellitus in a mouse model. Oral eugenol lowered blood glucose and insulin resistance of HFD/STZ-treated mice. Eugenol reduced HFD/STZ-induced muscle inflammation and prevented muscle weakness and atrophy. Eugenol administration significantly increased GLUT4 translocation and AMPK phosphorylation in skeletal muscle, thereby enhancing glucose uptake. By silencing the transient receptor potential vanilloid channel 1 (TRPV1) gene in C2C12 myotube cells, eugenol was found to increase intracellular Ca<sup>2+</sup> levels through TRPV1, which then activated calmodulin-dependent protein kinase-2 (CaMKK2) and affected AMPK protein phosphorylation. In conclusion, eugenol is a potential nutraceutical for preventing high-glucose-induced muscle impairments, which could be explained by its mediating effects on glucose absorption and inflammatory responses in the muscle.

## KEYWORDS

eugenol, diabetes, glucose, spices, muscle



## Introduction

Eugenol, the primary component of cinnamon, has anti-bacterial and anti-inflammatory functions and helps with metabolic problems (1). Eugenol can improve lipid metabolism disorders induced by a high-fat diet (HFD) by regulating oxidative stress (2). It has been demonstrated to improve liver gluconeogenesis and regulate blood glucose homeostasis through the Adenosine 5'-monophosphate (AMP)-activated protein kinase (AMPK) signaling pathway (3). Additionally, it is often used as a surgical anesthetic and plays a role in autoregulation (4). The anesthetic effect of eugenol depends on the transient receptor potential (TRP) signaling pathway, which mainly acts on transient receptor potential V1/V4/A1 (TRPV1, TRPV4, TRPA1). These TRP family targets regulate pain perception and temperature regulation (5). However, TRPV1 regulates energy metabolism, according to recent findings (6, 7).

Transient receptor potential vanilloid 1, also known as capsaicin receptor 1, can be activated by the specific binding of compounds with a vanillin group structure, such as capsaicin (8), piperine (9), and eugenol (10). Sensory nerves that express TRPV1 innervate all organs, including the hypothalamus (11) and skeletal muscle (12). TRPV1 protects diabetic liver against hyperglycemia and hyperlipidemia *via* OPA1 (13). Piperine may also impact glucose absorption in skeletal muscle by activating TRPV1 and influencing downstream glucose transporters (14). Recent studies have shown that capsaicin activates muscle cell ATP production and glucose oxidation *via* TRPV1 rather than the insulin pathway (15).

Although eugenol can activate TRPV1, it may have the same activation or inhibitory effects as capsaicin (16). TRPV1 acts as an ion channel in the cell membrane, controlling entry and exit of  $\text{Na}^+$ ,  $\text{K}^+$ , and  $\text{Ca}^{2+}$  (17).  $\text{Ca}^{2+}$  is a cellular regulatory messenger that is significantly associated with neural signaling (18), metabolism (19), and inflammatory responses (20). The flow of  $\text{Ca}^{2+}$  into cells may affect energy metabolism through the activation of downstream signaling pathways by calmodulin (21). On the other hand, diabetes leads to increased systemic inflammation, which in turn leads to complications (22, 23). Eugenol has been shown to regulate the level of inflammation in the body through signaling pathways such as NF- $\kappa$ B and COX-2 (24, 25). Therefore, in this study, we investigated whether eugenol could affect muscle function through muscle inflammation levels and glucose uptake in a high-fat-diet (HFD) plus streptozocin (STZ)-induced type 2 diabetes mellitus (T2DM) model. Furthermore, we examined the relationship between  $\text{Ca}^{2+}$  and AMPK signaling pathways and TRPV1 action *in vitro* to understand the possible mechanism of glucose regulation by eugenol.

## Materials and methods

### Animals and experimental design

A 6-week old male C57BL/6N mice were purchased from GemPharmatech (Nanjing, China). All experimental animals were kept in the Laboratory Animal Center of Jiangnan University under standardized conditions and were inspected and approved for experiments by the Animal Ethics Committee of Jiangnan University (JNU201804205).

Figure 1A displays the design of the animal experiment. After 2 weeks of acclimatization, the mice were divided into normal and high-fat feeding groups. The normal group mice ( $n = 10$ ) were fed a standard diet (LAD3001M, TROPIC, Nantong, China), and the high fat group mice ( $n = 50$ ) were fed a high-fat diet (HFD, 45% kcal from fat, TP23000, TROPIC, Nantong, China) for 8 weeks. The main formula of the feed is presented in Supplementary Table 2. After 8 weeks of feeding, mice in the HFD group were examined and selected for insulin resistance. Insulin-resistant mice received STZ (Solarbio, Beijing, China), whereas the normal group received a buffer solution. STZ was diluted in a 50 mM citric acid buffer, which was administered twice at a dosage rate of 35 mg/kg body weight, with a three-day gap between each administration (26, 27). After STZ injection, mice with fasting blood glucose (FBG) levels higher than 11 mM were selected for grouping and experimentation as T2DM model. They were randomly divided into four groups ( $n = 10$ ): (a) control group (Con, standard diet), (b) diabetes control group (DC, HFD/STZ), (c) low-dose eugenol group (DC + LE, HFD/STZ + 10 mg/kg/d eugenol), and (d) high-dose eugenol group (DC + HE, HFD/STZ + 20 mg/kg/d

eugenol). Eugenol were obtained from Macklin Technology (Shanghai, China). The eugenol dose was based on previous studies and our preliminary experiment on food intake (5–6 g/d/mice) after injecting STZ. Eugenol was administered to the mice through their feed for eight consecutive weeks.

## Oral glucose tolerance test and insulin tolerance test

All animals were fasted for 8 h, and blood glucose was measured as a baseline value. Blood glucose levels were monitored at 30, 60, 90, and 120 min following glucose gavage (1.8 g/kg body weight) or insulin injection (0.8 U/kg bodyweight). The area under the curve (AUC) for glucose content calculation was used as the result for OGTT and ITT. Blood samples were collected through the tail tip of mice in a quiet state, which was then cleaned promptly to stop bleeding.

## Tissue sample collection

After completion of the OGTT and ITT experiments, the mice met the expectations of variation within the ethical specifications, and all experimental animals were executed by cervical dislocation. All blood was collected into centrifuge tubes containing heparin and centrifuged at 4°C and  $3,000 \times g$  for 15 min to isolate the plasma. Muscle fractions were quickly dissected and divided into gastrocnemius muscles, placed in liquid nitrogen, and finally stored in a  $-80^{\circ}\text{C}$  refrigerator.

## Forelimb grip strength test

A Grip Strength Meter (Yiyan, Beijing, China) was used to test the forelimb grip strength of the mice. The mice naturally held to the rod on the dynamometer, which was moved horizontally and slowly until the mouse released the rod due to exhaustion.

## Body energy metabolism test

The body energy metabolism of mice was monitored by the crams system 1 week before slaughter. The main monitoring indicators included the 24 h respiratory exchange ratio (RER) value, autonomous activity, and energy consumption of mice. The RER value is the ratio of carbon dioxide production to oxygen consumption. Energy consumption was calculated by the following formula: Energy consumption =  $(3.815 + 1.232 \times \text{RER}) \times V_{O_2}$ . The amount of autonomous activity was calculated according to the number of times the infrared ray was broken in the horizontal and vertical

directions. Before the formal experiment, the mice were placed for 48 h in a metabolic cage, and the data obtained through monitoring for 24 h were used for statistical analysis. During the monitoring period, the mice were free to eat and drink water, and their food intake was monitored.

## Measurement of inflammatory cytokinesody

The Elisa kit's manufacturer's instructions (Huijia, Xiamen, China) were followed while measuring inflammatory cytokinesody.

## Histopathology and hematoxylin and eosin staining

Fixed in 4% paraformaldehyde for 24 h, tissues were embedded in paraffin and sliced in 5  $\mu\text{m}$  thick slices. TRPV1 antibody was used to stain slices for 24 h, which were treated with 3%  $\text{H}_2\text{O}_2$  in methanol for 15 min. Subsequently, the slices were washed, incubated with a secondary antibody for 1 h, and examined under a microscope to measure the intensity of immunostaining. Image analysis, including muscle fiber length measurements, were performed using the Image-Pro Plus (IPP) 6.0 software.

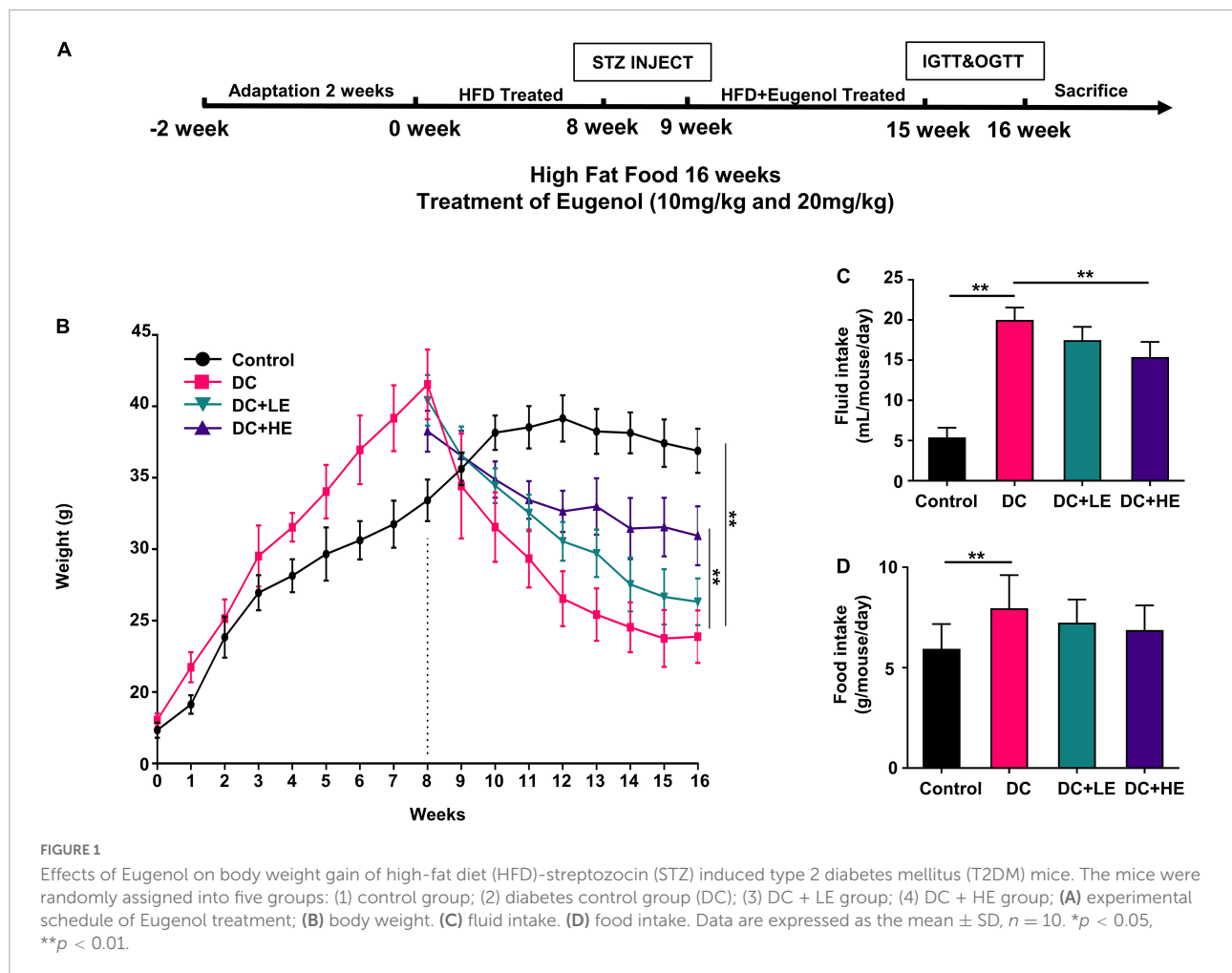
## Cell culture and viability assay

C2C12 cells (National Collection of Authenticated Cell Cultures, Shanghai, China) were grown in an incubator with 5%  $\text{CO}_2$  at  $37^{\circ}\text{C}$  in Dulbecco's modified Eagle's medium (DMEM, Gibco, CA, USA) with 10% fetal bovine serum (FBS, Gibco, CA, USA). The manufacturer's recommended methods for cell development were followed, and differentiation was achieved by switching the growth media to 2% horse serum, which was supplemented for 4 days.

Cytotoxicity was measured at different doses using a CCK-8 kit (Beyotime, Shanghai, China). The cells were seeded ( $4 \times 10^3$  cells per well) in 96-well plates. After 12 h of growth, the medium was replaced and treated with various doses of eugenol (25, 50, 100, 200, and 400  $\mu\text{M}$ ) dissolved in DMSO (0.5%). The absorbance value of cells at 480 nm was read to calculate the cell cytotoxicity results.

## Glucose uptake and glycogen synthesis

A 2-NBDG Glucose Test Kit (ab235976, Abcam) and a glycogen assay kit (ab65620, Abcam) were used to test glucose absorption in C2C12 cells. The cells were seeded



( $4 \times 10^3$  cells per well) in 96-well plates with 10% FBS in a 96-well black plate. After overnight incubation, cells were incubated with glucosamine (10 mM, Beyotime, Shanghai, China) for 6 h to construct the insulin resistance model. Eugenol (25, 50, 100, and 200  $\mu$ M) or 0.1% DMSO was used as the control in 100  $\mu$ l medium containing 100  $\mu$ g/ml 2-NBDG. After 6 h of incubation, the glucose uptake and glycogen of C2C12 cells was detected using a fluorescent microplate reader (Epoch, Bio-Tek, Winooski, VT, USA) (Glucose: excitation/emission = 485/535 nm, Glycogen: excitation/emission = 535/587 nm).

## RNAi transfection

For RNAi experiments, C2C12 cells were transfected with 100 nmol/L of si-TRPV1 (sense: 5'-GCGUCUAGCUGG UUGCACACU-3', antisense: 5'-GAGUAGCAACCGCCUU CAAGC-3', obtained from Genepharma, Shanghai, China) using Lipo8000 (Beyotime, Shanghai, China) transfection reagent 48 h before differentiation induction.

## Intracellular $Ca^{2+}$ detection

Each group's intracellular calcium ion density was calculated using a Fluo-4 AM probe. The cell density was  $4 \times 10^6$ /ml in each group. After glucosamine and eugenol treatment, 10  $\mu$ mol/L of Fluo-4 AM was applied to the cells. The cells were then grown in the dark for 30 min before being rinsed regularly with PBS buffer. Cells carrying calcium ions were found and calculated for each group using flow cytometry.

## Quantitative real-time polymerase chain reaction analysis

Briefly, we extracted and measured the gene expression levels of the samples using RNA extraction kits, cDNA reverse transcription kits, as well as RT-PCR kits. All kits were obtained from Vazyme (Nanjing, China). RT-PCR was performed using Quantagene q225 (Mona, Suzhou, China). Gene primers were

designed and synthesized by Genewiz (Shanghai, China) ([Supplementary Table 1](#)).

## Western-blot analysis

For western-blot experiments, all cell and tissue samples were lysed by RIPA solution (Beyotime, Shanghai, China), and protein denaturation was performed by loading buffer (Beyotime, Shanghai, China) after the protein concentration had been determined using a BCA kit (Thermo Fisher, Waltham, MA, USA). Protein samples were electrophoresed using polyacrylamide gels (Bio-Rad, Hercules, CA, USA) and transferred to a PVDF membrane by a semi-dry transfer method. After blocking, samples were treated with the target antibody for 12 h at 4°C. Antibodies were washed off after 1 h of incubation with secondary antibody. A staining kit (ECL chemiluminescence test kit, Vazyme, Nanjing, China), an Odyssey FC 2,800 imaging system (Licor, NE, USA) and the Image J software were used to analyze the results. The primary antibodies  $\beta$ -actin (#4970), NF- $\kappa$ B p65 (#8242), p-NF- $\kappa$ B p65 (#3033), p-AMPK $\alpha$  (#50081), AMPK $\alpha$  (#5832), and rabbit IgG were purchased from Cell Signaling Technology (Danvers, MA, USA). p-CAMKK $\beta$  (bs-6253R), CAMKK $\beta$  (bs-6253R), TRPV1 (bs-23926R), and GLUT4 (bs-0384R) were purchased from Bioss Antibodies Company (Beijing, China).

## Statistical analysis

Data are shown as the mean  $\pm$  standard error of the mean (SD). GraphPad Prism 6.0 was used to test for noteworthy mean value fluctuations through one-way ANOVA. Multiple comparisons were made using Tukey's test. A probability ( $p$ ) value less than 0.05 indicates statistically significant differences.

## Results

### Effect of eugenol treatment on body weight in high-fat diet/streptozocin-induced mice

After 8 weeks of treatment, as depicted in [Figure 1B](#), the DC group gained considerably more weight than the control group ( $p < 0.05$ ). The DC group weighed considerably less than the control group following STZ administration ( $p < 0.05$ ). During the 8-week treatment period following injection, the LE and HE groups exhibited a significant increase compared to the DC group ( $p < 0.05$ ). At 16 weeks, no

statistically differences were seen between the LE and HE groups. Significant increases in food consumption of 10.93% and water consumption of 39.81% were seen in the DC group ([Figures 1C,D](#)).

### Effect of eugenol treatment on respiratory exchange ratio, energy consumption, and activity of high-fat diet/streptozocin-induced mice

During 24 h monitoring, the DC group's RER, energy consumption, and activity were lower than those of the control group ([Figure 2](#),  $p < 0.01$ ). During day time, the RER value of the LE and HE groups significantly increased to more than those of the DC group ( $p < 0.05$ ), but there were no differences in energy consumption. However, at night, the activity and energy expenditure of mice after different doses of eugenol intervention were significantly higher than those of the DC group ( $p < 0.05$ ). HE mice used 1.2 times more energy than DC mice at night.

### Effect of eugenol supplementation on insulin resistance in high-fat diet/streptozocin-induced mice

Oral glucose tolerance test and insulin tolerance test determined the impact of eugenol on HFD/STZ-induced insulin resistance. In the LE and HE groups, fasting blood glucose levels were 24.86 and 40.77% lower than those in the DC group, respectively ([Figure 3A](#)). The serum insulin levels were 23.52% and 36.29% higher than those in the DC group, respectively ([Figure 3B](#)). Supplementation with eugenol effectively corrected the glucose intolerance (by 26.32%) and insulin sensitivity (by 22.41%) declines in T2DM mice ([Figures 3C,D](#)). In comparison to the DC group, fasting insulin levels in the LE and HE groups rose by 28.42 and 32.0%, respectively ([Figures 3E,F](#)).

### Effect of eugenol supplementation on gastrocnemius muscle mass to alleviate weight loss in high-fat diet/streptozocin-induced mice

To assess whether eugenol had an effect on muscle atrophy, we examined muscle tissue by H&E staining and measured muscle fiber size ([Figures 4A,B](#)). The results showed that the average length of muscle fibers in the DC group was 2-fold shorter compared to the control group. The mean length of

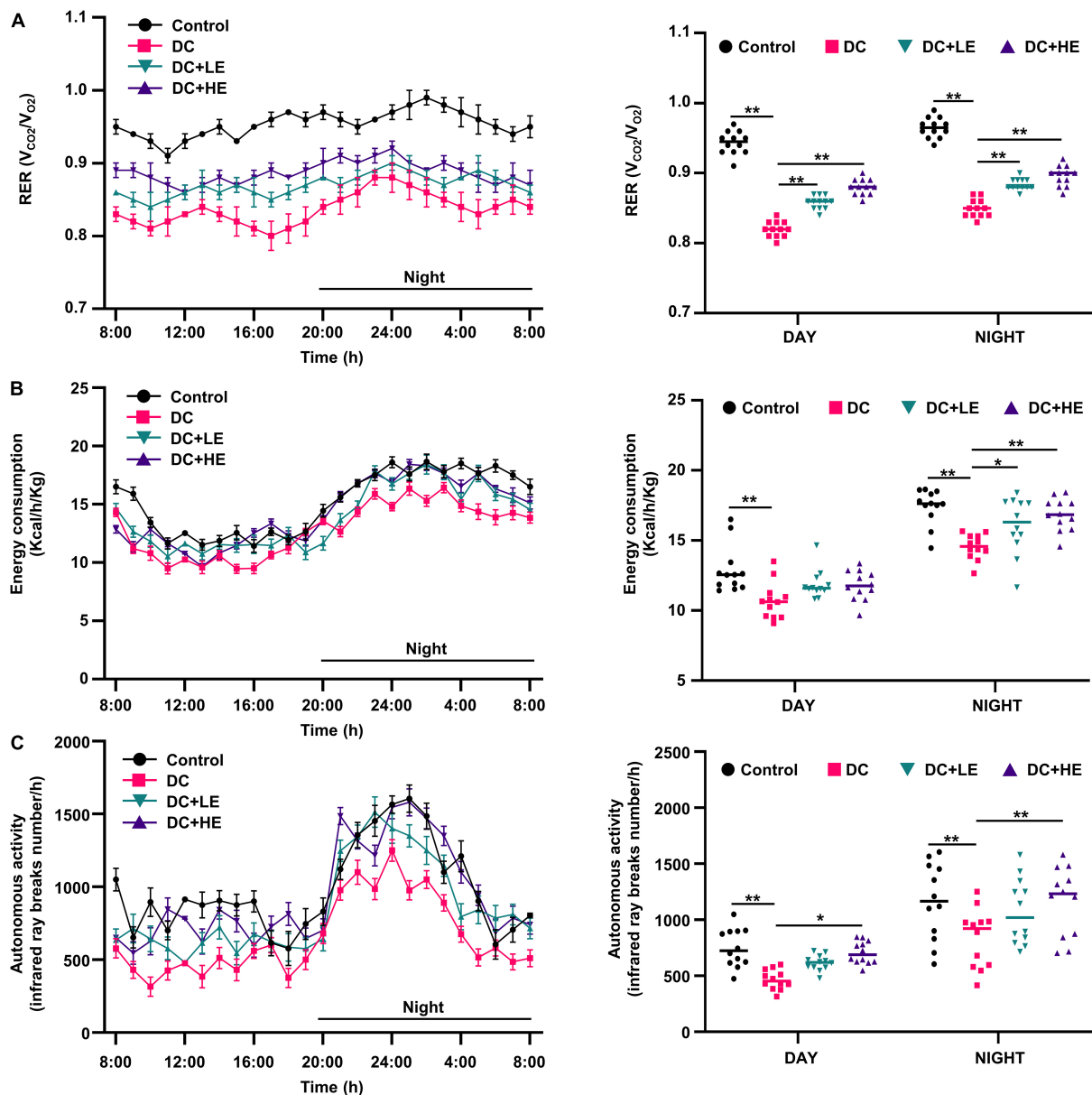


**FIGURE 2**  
 Effects of eugenol treatment on body energy metabolic status in type 2 diabetes mellitus (T2DM) mice. (A) 24 h respiratory exchange ratio (RER) dynamic monitoring curves of mice and mean values of daytime and nighttime respiratory exchange ratio (RER) of mice; (B) 24 h energy consumption dynamic monitoring curves of mice and mean values of daytime and nighttime energy consumption of mice; (C) 24 h autonomous activity dynamic monitoring curves of mice and mean values of daytime and nighttime autonomous activity of mice. Values for each group are expressed as mean  $\pm$  SD ( $n = 10$ ). \* $p < 0.05$ , \*\* $p < 0.01$ .

muscle fibers was significantly increased by 25% and 57% in the LE and HE groups, respectively, compared to the DC group ( $p < 0.01$ ). Muscle function was inversely proportional to muscle fiber size (24). **Figure 4C** shows that grip strength was 20% lower in the DC group than that of control group. In addition, the GA mass was significantly lower in the DC mice compared to the control group, while it was significantly higher in the HE group compared to the DC group (**Figure 4D**).

### Effect of eugenol supplementation on muscle protein synthesis gene expression and inflammatory cytokines via NF- $\kappa$ B phosphorylation in high-fat diet/streptozocin-induced mice

The increase in muscle weight and reversal of muscle fiber atrophy in mice suggest that eugenol may affect protein

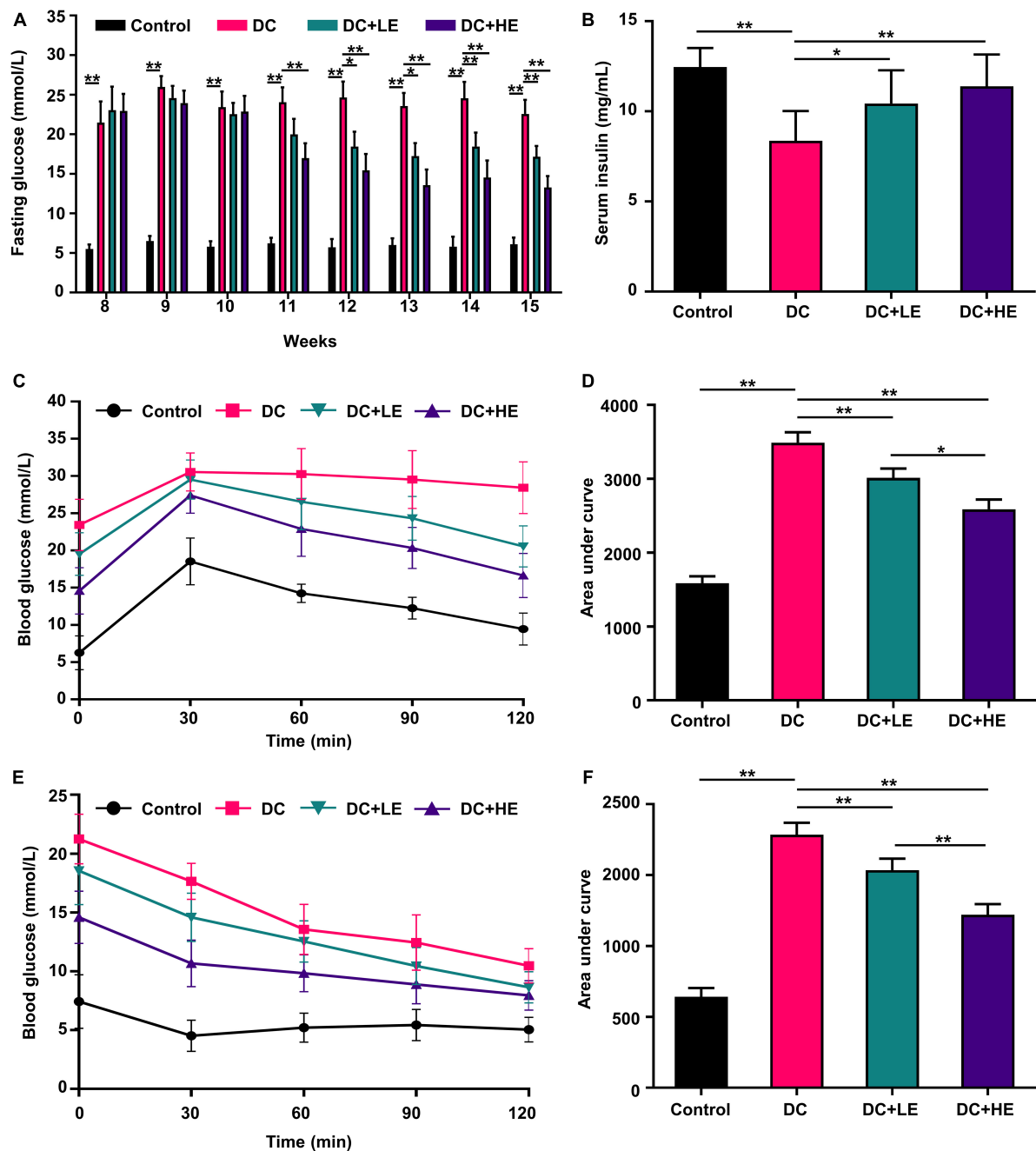


**FIGURE 3** Effects of eugenol on insulin resistance of the high-fat diet (HFD)-streptozocin (STZ)-induced type 2 diabetes mellitus (T2DM) mice. (A) Fasting glucose level. (B) Serum insulin. (C) Oral glucose tolerance test (OGTT). (D) Area under the curve (AUC) analyses for Oral glucose tolerance test (OGTT); (E) IGTT; (F) Area under the curve (AUC) analyses for IGTT; (E) fasting glucose level. Data are expressed as the mean ± SD n = 10. \*p < 0.05, \*\*p < 0.01.

synthesis and metabolism. We examined protein production and catabolism genes to explore protein changes. The expression levels of MuRF1 and atrogin-1 in the GA muscle increased in the DC group, and eugenol suppressed gene expression in the two dose groups (Figure 4F). Several studies have shown that muscle reduction in T2DM is associated with

inflammation (28). Therefore, we measured the levels of inflammatory cytokines in the muscle (Table 1). In DC muscles, IL-1, IL-6, and TNF- levels were considerably increased than in the control group. In the HE group, the three inflammatory cytokines decreased by 45, 26, and 17%. The level of anti-inflammatory cytokine IL-10

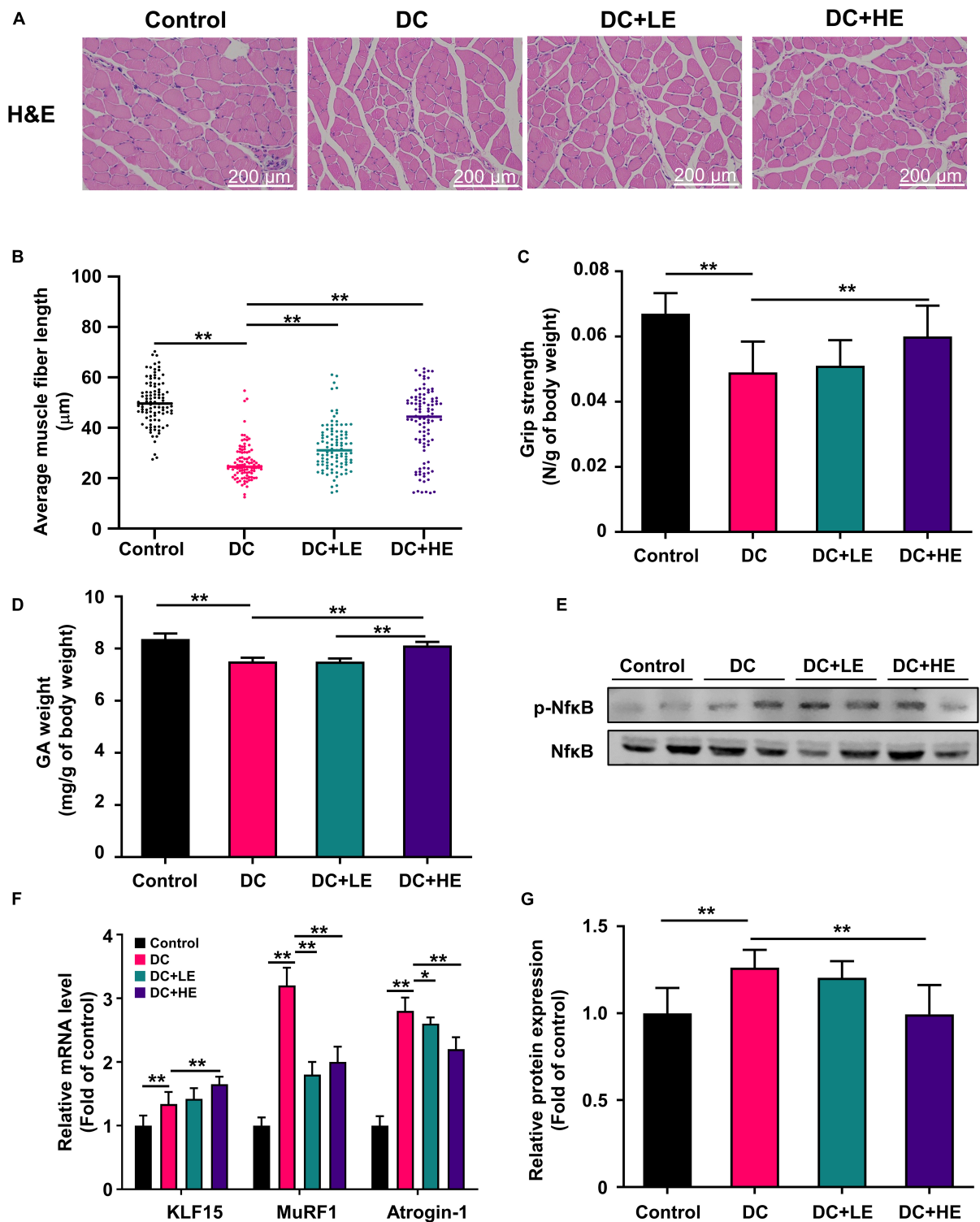


FIGURE 4

Effect of eugenol on muscle protein synthesis of the high-fat diet (HFD)-streptozocin (STZ)-induced type 2 diabetes mellitus (T2DM) mice. (A) H&E staining of gastrocnemius (GA) muscles section. (B) Grip strength was measured after 16 weeks of eugenol administration. (C) Effect of eugenol on gastrocnemius muscle fiber length in mice (100 samples per group). (D) The weights of gastrocnemius (GA) were measured right after sacrificing the mice and normalized to the body weight of each mouse. (E) mRNA levels of KLF15, MuRF1 and Atrogin-1 in the mice muscle. (F) Phospho-NFκB, NFκB, protein expression in muscle was analyzed by Western blotting. (G) Quantitative analysis of the Phospho-NFκB, NFκB, protein expression in muscle. Data are expressed as the mean ± SD,  $n = 10$ . \* $p < 0.05$ , \*\* $p < 0.01$ .



was significantly lower in the DC group, but increased significantly in the eugenol treatment group. We also examined the protein expression of NF- $\kappa$ B, a transcription factor associated with inflammation. The DC group exhibited significantly higher NF- $\kappa$ B phosphorylation than the control group, while the eugenol group had lower phosphorylation (Figures 4E,G).

### Effect of eugenol supplementation on skeletal muscle glycogen synthesis in high-fat diet/streptozocin-induced mice

Eugenol enhances skeletal muscle protein synthesis, and to investigate whether it is associated with improved muscle glucose utilization capacity, we measured glycogen in the skeletal muscle. PAS staining of skeletal muscle and glycogen tests showed that eugenol restored T2DM-related glycogen loss and raised muscle glycogen by 20% in the HE group compared to the DC group (Figures 5A,B).

### Eugenol increases skeletal muscle glucose uptake by promoting GLUT4 displacement through the AMPK signaling pathway

We measured the expression of the glucose transporter protein GLUT4 in the plasma membrane (PM) and cell lysate (Whole). The DC group had a lower PM GLUT4 protein expression than the control group. However, the expression of PM GLUT4/Whole GLUT4 in the eugenol intervention group was 1.2-fold and 1.5-fold higher than that in DC group at low and high doses, respectively (Figures 5D,F). We also measured AMPK protein expression associated with GLUT4 displacement. T2DM reduced AMPK protein phosphorylation, but eugenol increased it by 33.3% relative to the DC group (Figures 5D,E).

### Eugenol enhances the transient receptor potential vanilloid channel 1 expression in skeletal muscle

We detected the expression of TRPV1 in the skeletal muscle by immunohistochemistry and western blotting (Figures 5C,D). Compared to the T2DM model group, eugenol increased TRPV1 protein expression in the skeletal muscle 2.4-fold. Western-blot results showed that the expression levels of TRPV1 increased by 24 and 42% after the two doses of eugenol intervention compared to the DC group, respectively (Figures 5D,G).

### Eugenol enhances glucose uptake in mouse muscle C2C12 cells

We evaluated the effect of eugenol on glucosamine-induced insulin resistance in C2C12 cells. Eugenol showed no effect on C2C12 cell growth at 25–800  $\mu$ M, whereas 1,000  $\mu$ M decreased muscle cell proliferation (Figure 6A). Eugenol increased glucose uptake in cells at 25–200  $\mu$ M compared with insulin resistance (IR) cells. Stimulation with 100  $\mu$ M eugenol increased cellular glucose uptake approximately 1.6-fold, which was consistent with the effect of insulin stimulation in the positive control group (Figure 6B). Based on the above results, we chose a dose of 100  $\mu$ M eugenol for subsequent experiments.

### Eugenol increases the inward flow of $Ca^{2+}$ in C2C12 cells and upregulates the expression of the $Ca^{2+}$ transport protein calmodulin-dependent protein kinase-2

TRPV1, as an ion channel protein, is associated with intra- and extracellular  $Ca^{2+}$  flow. Therefore, we measured calcium ion changes in C2C12 cells after eugenol treatment using the fluorescent probe FLUO-8 AM to label  $Ca^{2+}$  in C2C12 cells. After 20 min of eugenol treatment, intracellular  $Ca^{2+}$  influx was higher than in the control group (Figure 6C). Quantitative analysis of fluorescent images showed that intracellular  $Ca^{2+}$  content increased approximately 3-fold after eugenol intervention compared to the control group (Figure 6C).

### Eugenol increases calcium transporter protein expression via $Ca^{2+}$ influx and stimulates the AMPK signaling pathway to increase glucose absorption in muscle cells

We determined the changes in the expression of CAMKK2, a calcium transport protein associated with cellular  $Ca^{2+}$  flow. The results showed that insulin stimulation did not alter CAMKK2 expression, while 50  $\mu$ M eugenol intervention significantly increased CAMMK2 expression by 50% compared to the IR group (Figure 6D). We examined the phosphorylation levels of AMPK, a downstream signal of CAMKK2 that may be activated and can contribute to the displacement of GLUT4. In terms of AMPK phosphorylation expression, 100  $\mu$ M eugenol, but not insulin, significantly increased AMPK phosphorylation levels 2.5-fold compared to the IR group (Figure 6F). In contrast, both insulin and eugenol increased the expression level of GLUT4 on PM, which was consistent with the glucose uptake results (Figure 6G), suggesting that eugenol and insulin differ in their mechanism of action of promoting cellular

TABLE 1 Effects of eugenol on the levels of inflammatory cytokine in the muscle of high-fat diet (HFD)-streptozocin (STZ) mice.

	IL-1 $\beta$ (ng/g protein)	IL-6 (ng/g protein)	TNF- $\alpha$ (ng/g protein)	IL-10 (ng/g protein)
Control	5.43 $\pm$ 0.67	4.86 $\pm$ 0.38	46.58 $\pm$ 8.66	107.6 $\pm$ 5.83
DC	10.05 $\pm$ 0.75**	9.75 $\pm$ 0.84**	121.5 $\pm$ 7.56**	50.43 $\pm$ 4.76**
DC + LE	7.04 $\pm$ 0.54##	8.95 $\pm$ 0.73	101.4 $\pm$ 8.68#	75.35 $\pm$ 3.98##
DC + HE	6.03 $\pm$ 0.46##	7.68 $\pm$ 0.69##	96.26 $\pm$ 6.52##	89.84 $\pm$ 4.13##

\*\* $p$  < 0.01, compared with the control group; # $p$  < 0.05, ## $p$  < 0.01, compared with the DC group.

glucose uptake. Similarly, we also examined changes in TRPV1 expression and found that insulin did not alter changes in intracellular TRPV1 expression, whereas eugenol significantly increased the level of TRPV1 protein expression at different doses (Figure 6E).

## Eugenol affects glucose uptake and calcium transport in muscle cells via transient receptor potential vanilloid channel

We knocked down TRPV1 (siTRPV1) in C2C12 cells to determine if the mechanism of action of eugenol in controlling glucose absorption is connected to TRPV1 expression. The results in Figure 7A show that the effect of insulin in enhancing glucose uptake in muscle cells did not differ significantly before and after the action of siTRPV1. In contrast, muscle glucose uptake was reduced by 60% after TRPV1 knockdown with eugenol. 100  $\mu$ M eugenol raised the glycogen level of IR-C2C12 cells, and siTRPV1 lowered it by 30% (Figure 7C). We used a spacious high-intensity system to capture the changes in Ca<sup>2+</sup> expression and found almost no increase in intracellular Ca<sup>2+</sup> in the TRPV1 knockdown group after 20 min of eugenol stimulation (Figure 7B).

## Eugenol affects Ca<sup>2+</sup> inward flow through transient receptor potential vanilloid channel 1 to regulate the CAMMK2-AMPK-GLUT4 signaling pathway, thus improving glucose utilization in muscle cells

To demonstrate that eugenol affects Ca<sup>2+</sup> and TRPV1-mediated downstream signaling, we determined the changes in protein expression in the signaling pathway after TRPV1 knockdown. Figures 7D,E indicate that siTRPV1 lowered TRPV1 expression, even with eugenol. The expression of the calcium transporter protein CAMMK2 decreased 3-fold after siTRPV1, even under eugenol stimulation (Figures 7D,F). The level of AMPK phosphorylation was significantly reduced after siTRPV1 and stimulation with 100  $\mu$ M eugenol (Figures 7D,G),

and the expression of GLUT4 on cell membranes was also significantly reduced (Figure 7D,H). These results show that eugenol may promote the displacement of GLUT4 to the cell membrane through TRPV1 by promoting inward calcium flow and activating the CAMMK-AMPK signaling pathway, ultimately leading to increased glucose uptake in skeletal muscle cells.

## Discussion

Type 2 diabetes mellitus is caused by a variety of factors, one of which is a high-fat diet that leads to decreased insulin sensitivity and, consequently, insulin resistance (29). We investigated mice treated with a high-fat diet and injected with STZ at week eight to create a T2DM mouse model. We found that the pathological symptoms of T2DM were relieved after the administration of eugenol, which led to a rapid loss of body weight in a short period owing to the inability of the mice to metabolize glucose by normal absorption and insufficient energy intake. It is likely that the diet and water intake of T2DM mice was affected by insufficient energy intake, and that the mice spontaneously increased fasting at the beginning of T2DM and increased water intake to eliminate excess glucose due to the high blood glucose level in the body (30). In this study, eugenol mitigated the weight loss associated with T2DM, and we demonstrated for the first time that eugenol enhanced water consumption, which was related with a reduction in blood glucose. Food intake did not change significantly after eugenol intervention, suggesting that eugenol does not improve T2DM symptoms in mice by restricting diet or energy intake, but may do so by enhancing energy utilization. The data of energy metabolism in mice over 24 h also demonstrated that eugenol increased the amount of energy metabolism in mice, particularly at night.

The main organs of glucose metabolism are the liver and muscles, and the liver maintains glucose homeostasis through glycolytic and gluconeogenic pathways. It has been observed that 40 mg/kg eugenol administration regulates hepatic gluconeogenesis via the AMPK signaling pathway, but 20 mg/kg eugenol had a limited effect on hepatic gluconeogenesis regulation (31). In the present study, we found that 10 mg/kg eugenol could still regulate fasting glucose, glucose tolerance, and insulin tolerance levels in T2DM mice.

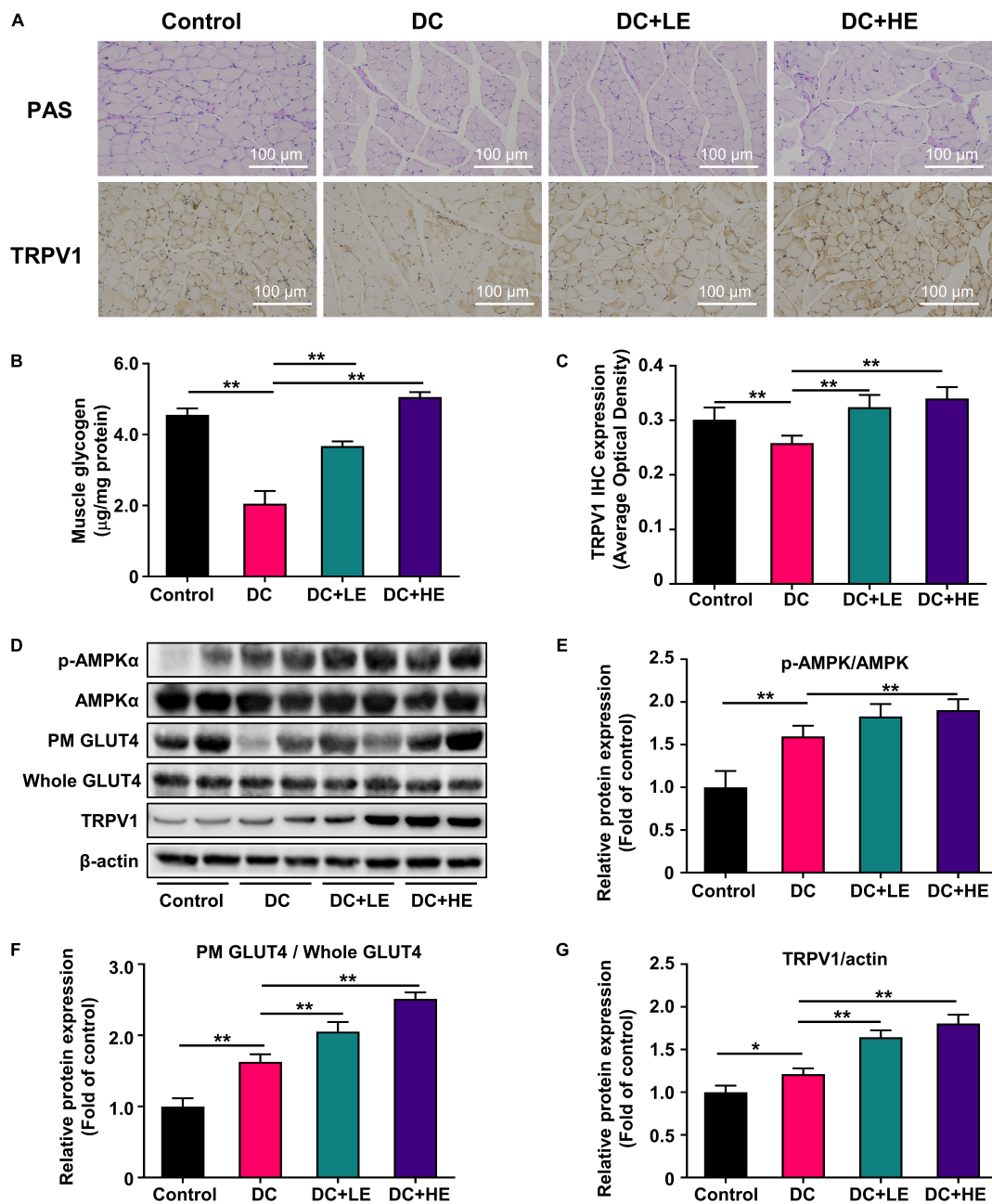
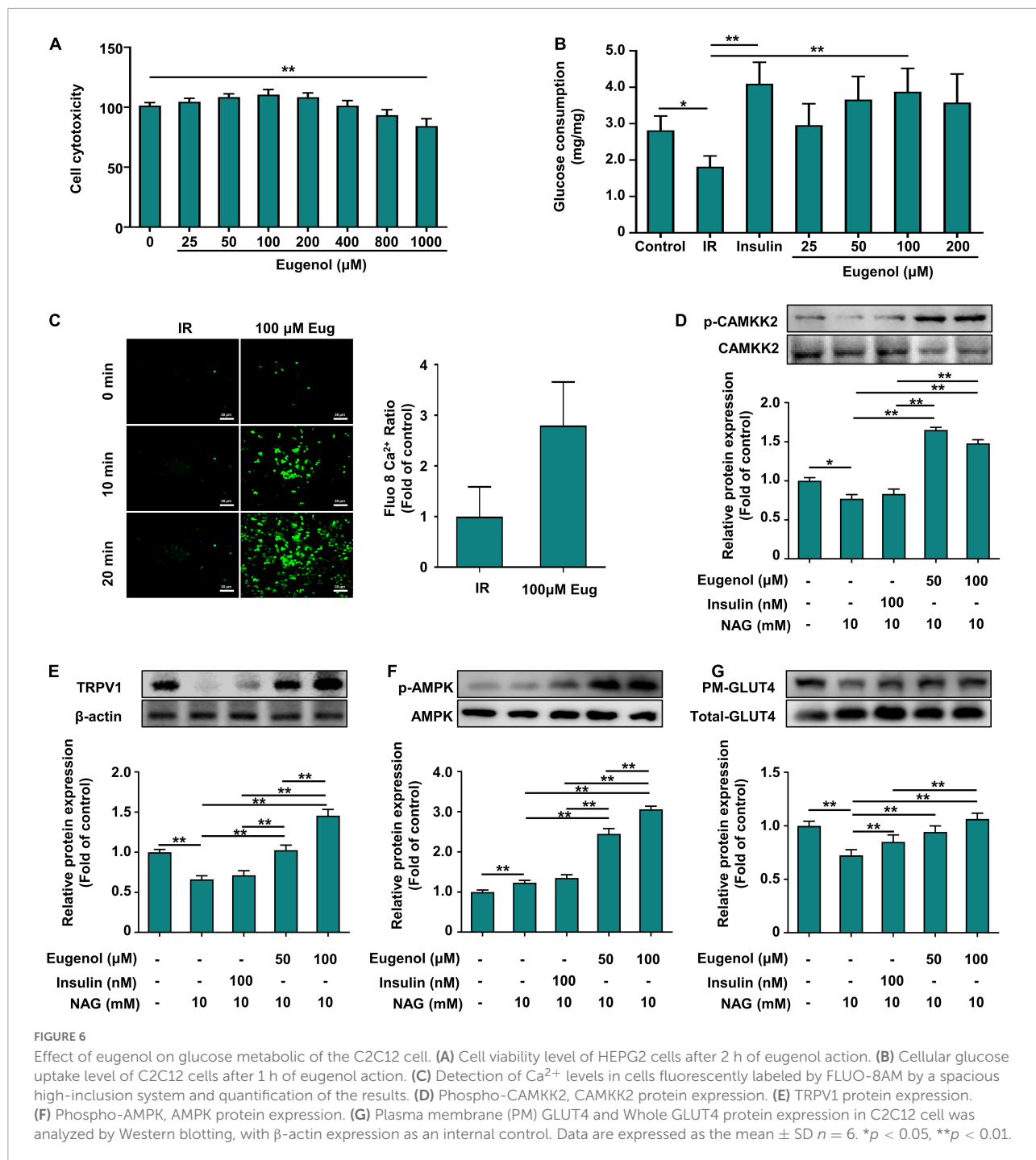


FIGURE 5

Effect of eugenol on muscle glucose metabolic of the high-fat diet (HFD)-streptozocin (STZ)-induced type 2 diabetes mellitus (T2DM) mice. (A) PAS staining of muscles section, and representative immunohistochemistry images for TRPV1 at 100× (B) muscle glycogen level of the mice. (C) IHC optical density score of TRPV1. (D) Phospho-AMPK, AMPK, plasma membrane (PM) GLUT4, Whole GLUT4 and TRPV1 protein expression in muscle was analyzed by Western blotting, with β-actin expression as an internal control. (E) Quantitative analysis of the Phospho-AMPK protein expression in muscle. (F) Quantitative analysis of the Plasma Membrane (PM) GLUT4 protein expression in muscle. (G) Quantitative analysis of the TRPV1 protein expression in muscle. Data are expressed as the mean ± SD, n = 10. \*p < 0.05, \*\*p < 0.01.

During 24 h of monitoring, eugenol increased respiratory exchange rates and energy metabolism in T2DM mice and significantly increased exercise levels at night. Skeletal muscles are an important organ for insulin action, and insulin resistance results in reduced glucose uptake, decreased exercise capacity, and eventually skeletal muscle atrophy (32, 33). It has been

reported that 35% of glucose is absorbed by muscles and produces energy (34). In the absence of insulin upstream signal Akt, skeletal muscles can maintain the normal level of glucose uptake through non-insulin signaling pathways to achieve a new balance of energy uptake and metabolism (34, 35).



The fact that eugenol enhanced muscle mass in mice with T2DM prompted us to investigate its influence on muscle synthesis and catabolic signaling. Type 2 diabetes has been shown to cause muscle atrophy due to a reduction in GA fiber volume, and grip strength in mice is strongly and positively linked with muscle fiber volume (36, 37). Hyperglycemia can influence the expression of genes involved in protein breakdown and synthesis when insulin deficiency causes a rise in blood

glucose levels (38). The increased expression of MuRF1 and atrogin-1 (protein degradation markers) in T2DM mice was downregulated at the mRNA level following eugenol treatment. Arogin-1 and MuRF1 gene expression levels are regulated by several transcription factors such as KLF15 and NF $\kappa$ B (39, 40). The intervention with eugenol had no effect on the gene expression of KLF15; however, it significantly decreased the phosphorylation level of NF $\kappa$ B. Studies have shown that NF $\kappa$ B

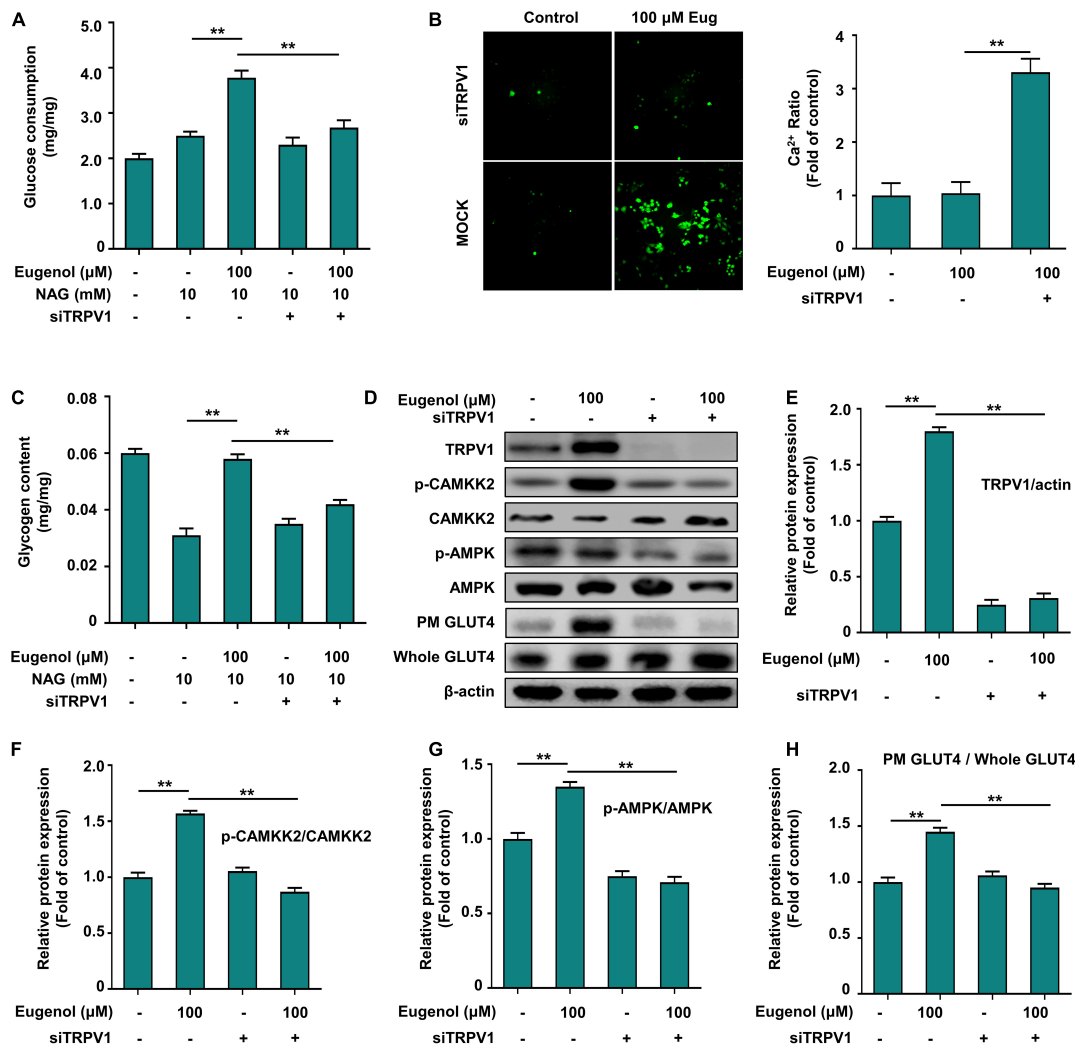


FIGURE 7

Eugenol affects glucose uptake in C2C12 cells *via* TRPV1. (A) Cellular glucose uptake level of C2C12 cells after 1 h of eugenol action with siTRPV1. (B) Detection of Ca<sup>2+</sup> levels in cells fluorescently labeled by FLUO-8AM by a spacious high-inclusion system. (C) Cellular glycogen level of C2C12 cells after 1 h of eugenol action with siTRPV1. (D) The result of western-blot. (E) TRPV1 protein expression. (F) Phospho-CAMKK2, CAMKK2 protein expression. (G) Phospho-AMPK, AMPK protein expression. (H) Plasma membrane (PM) GLUT4 and Whole GLUT4 protein expression in C2C12 cell was analyzed by Western blotting after siTRPV1 and eugenol action, with β-actin expression as an internal control. Data are expressed as the mean ± SD *n* = 6. \**p* < 0.05, \*\**p* < 0.01.

upregulates the muscle atrophy marker MURF1 by modulating inflammation levels rather than insulin levels (FOXO pathway); therefore, we hypothesized that eugenol also improves muscle atrophy by decreasing systemic inflammation, which has been demonstrated on different animals in several previous studies (41, 42).

However, the increase in skeletal muscle protein may stem from increased energy absorption. The intervention with eugenol significantly improved glucose absorption and glycogen production in the skeletal muscle of T2DM mice. Glucose absorption could provide the energy required for muscle protein synthesis, whereas the glycogen reserves could enhance exercise capacity in mice (43). In this work, eugenol increased GLUT4

translocation to the plasma membrane *via* the AMPK route, but not the insulin pathway. Some natural compounds can regulate cellular energy metabolism through activation of downstream AMPK phosphorylation by CAMKK2 (44, 45). Our results demonstrated that eugenol intervention increased cellular Ca<sup>2+</sup> inflow and CAMKK2 expression.

Transient receptor potential vanilloid channel is a ligand-gated, non-selective cation channel, whose activation leads to Ca<sup>2+</sup> influx (46). Both the plasma membrane and the endoplasmic reticulum express TRPV1. It is unclear how eugenol affects TRPV1, but molecular docking experiments indicate that its vanilloid group can attach to TRPV1 as effectively as capsaicin (41). In obesity studies, activation of

TRPV1 is detrimental because high fat leads to enhanced TRPV1 expression (47). Like capsaicin, eugenol may also act on TRPV1 with a dose-dependent bidirectional effect of activation followed by desensitization (48, 49). However, there are also many reports showing that TRPV1 activation can improve metabolic syndrome (50–52). Our evidence supports this view, and our results demonstrated that TRPV1 activation promotes inward calcium flow, which in turn induces enhanced muscle glucose uptake. It is possible that our dose and time of administration did not reach a desensitized state. In addition, eugenol helps restore energy metabolic homeostasis in hyperglycemic mice, as prolonged increased muscle glucose uptake is not beneficial. We hypothesized that after blood glucose levels are stabilized, eugenol changes the calcium ion flow to reach a new equilibrium, which is consistent with the mechanisms in which the brain regulates neural signaling through calcium ions (53, 54). To achieve this balance, activation and inhibition of TRPV1 as an ion channel may be a key regulatory factor.

In conclusion, we suggest that eugenol increases intracellular  $\text{Ca}^{2+}$  levels *via* TRPV1, followed by the activation of CaMKK $\beta$  and enhanced AMPK phosphorylation, leading to enhanced muscle glucose uptake and triggering an improvement in systemic energy metabolism. Thus, eugenol may be a viable phytochemical for avoiding glucose metabolism deficiencies caused by metabolic disorders.

## Data availability statement

The raw data supporting the conclusions of this article will be made available by the authors, without undue reservation.

## Ethics statement

This animal study was reviewed and approved by Jiangnan University Animal Ethics Committee.

## Author contributions

YJ and GL: conceptualization, project administration, and funding acquisition. YJ, CF, YS, and GL: methodology. YJ, CF, and GL: formal analysis. YJ, CF, and YS: investigation.

## References

1. Sartorius T, Peter A, Schulz N, Drescher A, Bergheim I, Machann J, et al. Cinnamon extract improves insulin sensitivity in the brain and lowers liver fat in mouse models of obesity. *PLoS One*. (2014) 9:e92358. doi: 10.1371/journal.pone.0092358

YJ and CF: data curation. YJ, CF, and XK: writing—original draft preparation. YJ, CF, YS, GL, and XK: writing—review and editing. YS and GL: supervision. All authors read and agreed to the published version of the manuscript.

## Funding

This work was financially supported by Postgraduate Research and Practice Innovation Program of Jiangsu Province (KYCX18-1769).

## Acknowledgments

We thank Dr. Xu Ruijie from Jiangnan University for her contribution to the conception and design of the images in this article. We also thank Editage ([www.editage.cn](http://www.editage.cn)) for English language editing.

## Conflict of interest

The authors declare that the research was conducted in the absence of any commercial or financial relationships that could be construed as a potential conflict of interest.

## Publisher's note

All claims expressed in this article are solely those of the authors and do not necessarily represent those of their affiliated organizations, or those of the publisher, the editors and the reviewers. Any product that may be evaluated in this article, or claim that may be made by its manufacturer, is not guaranteed or endorsed by the publisher.

## Supplementary material

The Supplementary Material for this article can be found online at: <https://www.frontiersin.org/articles/10.3389/fnut.2022.1039753/full#supplementary-material>

2. Bezerra DP, Militão GCG, de Moraes MC, de Sousa DP. The dual antioxidant/prooxidant effect of eugenol and its action in cancer development and treatment. *Nutrients*. (2017) 9:1367. doi: 10.3390/nu9121367

3. Ali S, Prasad R, Mahmood A, Routray I, Shinkafi TS, Sahin K, et al. Eugenol-rich fraction of *Syzygium Aromaticum* (Clove) reverses biochemical and histopathological changes in liver cirrhosis and inhibits hepatic cell proliferation. *J Cancer Prevent.* (2014) 19:288–300. doi: 10.15430/jcp.2014.19.4.288
4. Islam SS, Al-Sharif I, Sultan A, Al-Mazrou A, Remmal A, Aboussekhra A. Eugenol potentiates cisplatin anti-cancer activity through inhibition of aldehyde dehydrogenase 1A1 and 1A2-dependent and -independent pathways. *Mol Carcinogen.* (2018) 57:333–46. doi: 10.1002/mc.22758
5. Cao Z, Balasubramanian A, Marrelli SP. Pharmacologically induced hypothermia via Trpv1 channel agonism provides neuroprotection following ischemic stroke when initiated 90 min after reperfusion. *Am J Physiol Regul Integr Comp Physiol.* (2014) 306:R149–56. doi: 10.1152/ajpregu.00329.2013
6. Li M, Zhang CS, Zong Y, Feng JW, Ma T, Hu M, et al. Transient receptor potential V channels are essential for glucose sensing by aldolase and ampk. *Cell Metab.* (2019) 30:508–24.e12. doi: 10.1016/j.cmet.2019.05.018
7. Gifford JR, Ives SJ, Park SY, Andtbacka RH, Hyngstrom JR, Mueller MT, et al. A1- and A2-adrenergic responsiveness in human skeletal muscle feed arteries: the role of trpv ion channels in heat-induced sympatholysis. *Am J Physiol Heart Circ Physiol.* (2014) 307:H1288–97. doi: 10.1152/ajpheart.00068.2014
8. Bao Z, Dai X, Wang P, Tao Y, Chai D. Capsaicin induces cytotoxicity in human osteosarcoma Mg63 cells through Trpv1-dependent and -independent pathways. *Cell Cycle.* (2019) 18:1379–92. doi: 10.1080/15384101.2019.1618119
9. Dong Y, Yin Y, Vu S, Yang F, Yarov-Yaroyov V, Tian Y, et al. A distinct structural mechanism underlies trpv1 activation by piperine. *Biochem Biophys Res Commun.* (2019) 516:365–72. doi: 10.1016/j.bbrc.2019.06.039
10. Harb AA, Bustanji YK, Almasri IM, Abdalla SS. Eugenol reduces ldl cholesterol and hepatic steatosis in hypercholesterolemic rats by modulating trpv1 receptor. *Sci Rep.* (2019) 9:14003. doi: 10.1038/s41598-019-50352-4
11. Molinas AJR, Desmoulin LD, Hamling BV, Butcher SM, Anwar IJ, Miyata K, et al. Interaction between trpv1-expressing neurons in the hypothalamus. *J Neurophysiol.* (2019) 121:140–51. doi: 10.1152/jn.00004.2018
12. Hurtado-Zavala JL, Ramachandran B, Ahmed S, Halder R, Bolleyer C, Awasthi A, et al. Trpv1 regulates excitatory innervation of olm neurons in the hippocampus. *Nat Commun.* (2017) 8:15878. doi: 10.1038/ncomms15878
13. Wang T, Chen Y, Li Y, Wang Z, Qiu C, Yang D, et al. Trpv1 protect against hyperglycemia and hyperlipidemia induced liver injury via opa1 in diabetes. *Tohoku J Exp Med.* (2022) 256:131–9. doi: 10.1620/tjem.256.131
14. Stanford KR, Hadley SH, Barannikov I, Ajmo JM, Bahia PK, Taylor-Clark TE. Antimycin a-induced mitochondrial dysfunction activates vagal sensory neurons via ros-dependent activation of trpa1 and ros-independent activation of trpv1. *Brain Res.* (2019) 1715:94–105. doi: 10.1016/j.brainres.2019.03.029
15. Vahidi Ferdowsi P, Ahuja KDK, Beckett JM, Myers S. Trpv1 activation by capsaicin mediates glucose oxidation and atp production independent of insulin signalling in mouse skeletal muscle cells. *Cells.* (2021) 10:1560. doi: 10.3390/cells10061560
16. McArthur JR, Finol-Urdaneta RK, Adams DJ. Analgesic transient receptor potential vanilloid-1-active compounds inhibit native and recombinant t-type calcium channels. *Br J Pharmacol.* (2019) 176:2264–78. doi: 10.1111/bph.14676
17. Vangael L, Voets T. Transient receptor potential channels and calcium signaling. *Cold Spring Harb Perspect Biol.* (2019) 11:a035048. doi: 10.1101/cshperspect.a035048
18. Braunewell KH, Klein-Szanto AJ. Visinin-like proteins (Vsnls): interaction partners and emerging functions in signal transduction of a subfamily of neuronal Ca2+ -sensor proteins. *Cell Tissue Res.* (2009) 335:301–16. doi: 10.1007/s00441-008-0716-3
19. Belosludtsev KN, Belosludtseva NV, Dubinin MV. Diabetes mellitus, mitochondrial dysfunction and Ca(2+)-dependent permeability transition pore. *Int J Mol Sci.* (2020) 21:6559. doi: 10.3390/ijms21186559
20. Chen Q, Zhou Y, Zhou L, Fu Z, Yang C, Zhao L, et al. Trpc6-dependent Ca(2+) signaling mediates airway inflammation in response to oxidative stress via erk pathway. *Cell Death Dis.* (2020) 11:170. doi: 10.1038/s41419-020-2360-0
21. Hou L, Jiang F, Huang B, Zheng W, Jiang Y, Cai G, et al. Dihydromyricetin resists inflammation-induced muscle atrophy via ryanodine receptor-camk-ampk signal pathway. *J Cell Mol Med.* (2021) 25:9953–71. doi: 10.1111/jcmm.16810
22. Yang J, Wei Y, Zhao T, Li X, Zhao X, Ouyang X, et al. Magnolol effectively ameliorates diabetic peripheral neuropathy in mice. *Phytomedicine.* (2022) 107:154434. doi: 10.1016/j.phymed.2022.154434
23. Chen J, Meng X. Aronia melanocarpa anthocyanin extracts improve hepatic structure and function in high-fat diet-streptozotocin-induced t2dm mice. *J Agric Food Chem.* (2022) 70:11531–43. doi: 10.1021/acs.jafc.2c03286
24. Wang K, Chen D, Yu B, He J, Mao X, Huang Z, et al. Eugenol alleviates transmissible gastroenteritis virus-induced intestinal epithelial injury by regulating Nf-Kb signaling pathway. *Front Immunol.* (2022) 13:921613. doi: 10.3389/fimmu.2022.921613
25. das Chagas Pereira de Andrade F, Mendes AN. Computational analysis of eugenol inhibitory activity in lipoxygenase and cyclooxygenase pathways. *Sci Rep.* (2020) 10:16204. doi: 10.1038/s41598-020-73203-z
26. Zhang C, Deng J, Liu D, Tuo X, Xiao L, Lai B, et al. Nuciferine ameliorates hepatic steatosis in high-fat diet/streptozotocin-induced diabetic mice through a Ppara/Pparγ coactivator-1α pathway. *Br J Pharmacol.* (2018) 175:4218–28. doi: 10.1111/bph.14482
27. Nath S, Ghosh SK, Choudhury YA. Murine model of type 2 diabetes mellitus developed using a combination of high fat diet and multiple low doses of streptozotocin treatment mimics the metabolic characteristics of type 2 diabetes mellitus in humans. *J Pharmacol Toxicol Methods.* (2017) 84:20–30. doi: 10.1016/j.vascn.2016.10.007
28. Marcelo KL, Ribar T, Means CR, Tsimelzon A, Stevens RD, Ilkayeva O, et al. Research resource: roles for calcium/calmodulin-dependent protein kinase kinase 2 (CAMKK2) in systems metabolism. *Mol Endocrinol.* (2016) 30:557–72. doi: 10.1210/me.2016-1021
29. Galicia-García U, Benito-Vicente A, Jebari S, Larrea-Sebal A, Siddiqi H, Uribe KB, et al. Pathophysiology of type 2 diabetes mellitus. *Int J Mol Sci.* (2020) 21:6275. doi: 10.3390/ijms21176275
30. Sedaghat G, Montazerifar F, Keykhaie MA, Karajibani M, Shourestani S, Dashipour A. Effect of pre-meal water intake on the serum levels of copeptin, glycemic control, lipid profile and anthropometric indices in patients with type 2 diabetes mellitus: a randomized, controlled trial. *J Diabet Metab Disord.* (2021) 20:171–7. doi: 10.1007/s40200-020-00724-9
31. Jeong KJ, Kim DY, Quan HY, Jo HK, Kim GW, Chung SH. Effects of Eugenol on Hepatic Glucose Production and Ampk Signaling Pathway in Hepatocytes and C57bl/6j Mice. *Fitoterapia.* (2014) 93:150–62. doi: 10.1016/j.fitote.2013.12.023
32. Calderón-DuPont D, Torre-Villalvazo I, Díaz-Villaseñor A. Is insulin resistance tissue-dependent and substrate-specific? The role of white adipose tissue and skeletal muscle. *Biochimie* (2022). [Epub ahead of print]. doi: 10.1016/j.biochi.2022.08.021
33. Seo DH, Suh YJ, Cho Y, Ahn SH, Seo S, Hong S, et al. Effect of low skeletal muscle mass and sarcopenic obesity on chronic kidney disease in patients with type 2 diabetes. *Obesity.* (2022) 30:2034–43. doi: 10.1002/oby.23512
34. Jaiswal N, Gavin MG, Quinn WJ III, Luongo TS, Gelfer RG, Baur JA, et al. The role of skeletal muscle akt in the regulation of muscle mass and glucose homeostasis. *Mol Metab.* (2019) 28:1–13. doi: 10.1016/j.molmet.2019.08.001
35. Bai J, Zhang S, Cao J, Sun H, Mang Z, Shen WL, et al. Hernandezine, a natural herbal alkaloid, ameliorates type 2 diabetes by activating ampk in two mouse models. *Phytomedicine.* (2022) 105:154366. doi: 10.1016/j.phymed.2022.154366
36. Armstrong RB, Gollnick PD, Ianzzo CD. Histochemical properties of skeletal muscle fibers in streptozotocin-diabetic rats. *Cell Tissue Res.* (1975) 162:387–94. doi: 10.1007/bf00220185
37. Ciciliot S, Rossi AC, Dyar KA, Blaauw B, Schiaffino S. Muscle type and fiber type specificity in muscle wasting. *Int J Biochem Cell Biol.* (2013) 45:2191–9. doi: 10.1016/j.biocel.2013.05.016
38. Wang D, Sun H, Song G, Yang Y, Zou X, Han P, et al. Resveratrol improves muscle atrophy by modulating mitochondrial quality control in stz-induced diabetic mice. *Mol Nutr Food Res.* (2018) 62:e1700941. doi: 10.1002/mnfr.201700941
39. Choi HJ, Yeon MH, Jun HS. Schisandrae chinensis fructus extract ameliorates muscle atrophy in streptozotocin-induced diabetic mice by downregulation of the creb-klf15 and autophagy-lysosomal pathways. *Cells.* (2021) 10:2283. doi: 10.3390/cells10092283
40. Zhang N, Valentine JM, Zhou Y, Li ME, Zhang Y, Bhattacharya A, et al. Sustained Nfkb inhibition improves insulin sensitivity but is detrimental to muscle health. *Aging Cell.* (2017) 16:847–58. doi: 10.1111/acel.12613
41. Al-Trad B, Alkhateeb H, Alsmadi W, Al-Zoubi M. Eugenol ameliorates insulin resistance, oxidative stress and inflammation in high fat-diet/streptozotocin-induced diabetic rat. *Life Sci.* (2019) 216:183–8. doi: 10.1016/j.lfs.2018.11.034
42. Monteschio JO, Vargas-Junior FM, Almeida FLA, Pinto LAM, Kaneko IN, Almeida AA, et al. The effect of encapsulated active principles (Eugenol, Thymol and Vanillin) and clove and rosemary essential oils on the structure, collagen content, chemical composition and fatty acid profile of nellore heifers muscle. *Meat Sci.* (2019) 155:27–35. doi: 10.1016/j.meatsci.2019.04.019
43. Hingst JR, Bruhn L, Hansen MB, Rosschou MF, Birk JB, Fentz J, et al. Exercise-induced molecular mechanisms promoting glycogen supercompensation in human skeletal muscle. *Mol Metab.* (2018) 16:24–34. doi: 10.1016/j.molmet.2018.07.001

44. Antonia RJ, Baldwin AS. Ikk promotes cytokine-induced and cancer-associated ampk activity and attenuates phenformin-induced cell death in lkb1-deficient cells. *Sci Signal*. (2018) 11:eaan5850. doi: 10.1126/scisignal.aan5850
45. Lan F, Weikel KA, Cacicedo JM, Ido Y. Resveratrol-induced amp-activated protein kinase activation is cell-type dependent: lessons from basic research for clinical application. *Nutrients*. (2017) 9:751. doi: 10.3390/nu9070751
46. Froghi S, Grant CR, Tandon R, Quaglia A, Davidson B, Fuller B. New insights on the role of trp channels in calcium signalling and immunomodulation: review of pathways and implications for clinical practice. *Clin Rev Allergy Immunol*. (2021) 60:271–92. doi: 10.1007/s12016-020-08824-3
47. Lee E, Jung DY, Kim JH, Patel PR, Hu X, Lee Y, et al. Transient receptor potential vanilloid type-1 channel regulates diet-induced obesity, insulin resistance, and leptin resistance. *Faseb J*. (2015) 29:3182–92. doi: 10.1096/fj.14-268300
48. Shuba YM. Beyond neuronal heat sensing: diversity of trpv1 heat-capsaicin receptor-channel functions. *Front Cell Neurosci*. (2020) 14:612480. doi: 10.3389/fncel.2020.612480
49. Takahashi K, Yoshida T, Wakamori M. Mode-selective inhibitory effects of eugenol on the mouse trpv1 channel. *Biochem Biophys Res Commun*. (2021) 556:156–62. doi: 10.1016/j.bbrc.2021.03.126
50. Baskaran P, Krishnan V, Ren J, Thyagarajan B. Capsaicin induces browning of white adipose tissue and counters obesity by activating trpv1 channel-dependent mechanisms. *Br J Pharmacol*. (2016) 173:2369–89. doi: 10.1111/bph.13514
51. Baskaran P, Krishnan V, Fettel K, Gao P, Zhu Z, Ren J, et al. Trpv1 activation counters diet-induced obesity through sirtuin-1 activation and prdm-16 deacetylation in brown adipose tissue. *Int J Obes*. (2017) 41:739–49. doi: 10.1038/ijo.2017.16
52. Moraes RDA, Webb RC, Silva DF. Vascular dysfunction in diabetes and obesity: focus on trp channels. *Front Physiol*. (2021) 12:645109. doi: 10.3389/fphys.2021.645109
53. Ma L, Mu Y, Zhang Z, Sun Q. Eugenol promotes functional recovery and alleviates inflammation, oxidative stress, and neural apoptosis in a rat model of spinal cord injury. *Restor Neurol Neurosci*. (2018) 36:659–68. doi: 10.3233/rnn-180826
54. Tan N, Shi J, Xu L, Zheng Y, Wang X, Lai N, et al. Lateral hypothalamus calcium/calmodulin-dependent protein kinase II  $\alpha$  neurons encode novelty-seeking signals to promote predatory eating. *Research*. (2022) 2022:9802382. doi: 10.34133/2022/9802382